Proc. Natl. Acad. Sci. USA
Vol. 81, pp. 771–775, February 1984
Cell Biology

Interference of GTP hydrolysis in the mechanism of microtubule assembly: An experimental study

(tubulin/steady-state polymer/nonlinear flux/Monte Carlo theory)

MARIE-FRANCE CARLIER*, TERRELL L. HILL†, AND YI-DER CHEN†

*Laboratoire d'Enzymologie, Centre National de la Recherche Scientifique, 91190 Gif-sur-Yvette, France; and †Laboratory of Molecular Biology, National Institute of Arthritis, Diabetes, and Digestive and Kidney Diseases, National Institutes of Health, Bethesda, MD 20205

Contributed by Terrell L. Hill, October 13, 1983

ABSTRACT **This paper reports an experimental study of the interference of GTP hydrolysis in the mechanism of microtubule assembly, following the model and theory previously published [Hill, T. L. & Carlier, M.-F. (1983) *Proc. Natl. Acad. Sci. USA* 80, 7234–7238]. Results from dilution experiments show that microtubules depolymerize faster below the critical concentration than expected with a reversible polymerization model. The experimental plot of flux versus tubulin concentration exhibits a slope discontinuity at the critical concentration, in agreement with the theory. Theoretical points calculated by the Monte Carlo method can be fitted qualitatively to the data. A consequence of this peculiar dynamic behavior of microtubules is that the ratio of tubulin dissociation and association rate constants measured, respectively, below and above the critical concentration does not yield the true value of the critical concentration. It is emphasized that the presence of GTP at microtubule ends is necessary to maintain the stability of the polymer.**

It is striking that two essential polymer components of the cytoskeleton of eukaryotic cells, actin filaments and microtubules (MTs), share many structural and physicochemical properties. In particular, the NTP bound to the protomer (ATP to actin, GTP to tubulin) undergoes hydrolysis during polymerization (1–3). NTP hydrolysis is also associated with maintenance of the polymers. Indeed, in the presence of low concentrations of GTP, MTs eventually depolymerize (4) and GDP is unable to promote polymerization (2). Therefore, actin filaments and MTs must be considered as steady-state polymers. However, GTP hydrolysis associated with MT assembly does not appear necessary for polymerization because hydrolysis is a monomolecular kinetic process uncoupled from polymerization (5), a result also more recently reported on actin (6, 7). Correlatively, MTs can be obtained and stabilized in the presence of nonhydrolyzable analogs of GTP (8) and thus be maintained in an equilibrium state.

Although GTP hydrolysis is involved in MT assembly and steady state, until now Oosawa's model, which applies to equilibrium polymers—i.e., those undergoing linear reversible polymerization—satisfactorily accounted for the kinetic and thermodynamic data for MT assembly (4, 9).

In an effort to explore the consequences of nucleotide hydrolysis in the polymerization process, Wegner first developed a model (10) pointing to the possibility of "head-to-tail polymerization" driven by ATP hydrolysis in actin polymerization. The same phenomenon was observed experimentally on MTs and called "treadmilling" by Margolis and Wilson (11).

Possible implications of treadmilling in the regulation of MTs *in vivo* have been suggested (12–15). On the basis of Wegner's model, the thermokinetic theory of MT and actin polymerization has been developed (16). In this model, GTP hydrolysis is tightly coupled to the polymerization process. As a consequence, only GDP is bound to the polymer and the critical concentrations (which may be different at the two ends) can be expressed as the ratio of the rate constants for dissociation of tubulin-GDP and association of tubulin-GTP. Yet the theoretical curve of the rate of growth of the polymer versus tubulin concentration remains linear as in the case of an equilibrium polymer.

However, several experimental observations have been made that are in opposition to Wegner's model, in the case of MTs. (*i*) The fact that GTP hydrolysis accompanying assembly occurs in a step subsequent to the polymerization process results in the formation of a steady-state cap of GTP at the ends of MTs (17). An approximate analytical formulation of the properties of this cap has been reported (16). (*ii*) Tubulin present at the very end of MTs can bind either GTP or GDP, and this affects the rate of growth; typically an elongating site having GDP bound is blocked and cannot bind tubulin subunits (18). Relaxation studies (19) lead to the same conclusion.

The presence of GDP at the very end can result from the exchange of nucleotide, from the binding of a tubulin-GDP subunit, or from GTP hydrolysis. These data (18) suggest that not only is GTP hydrolysis not necessary for polymerization but it inhibits polymerization. It is likely that the rate of dissociation of tubulin subunits also depends on whether GTP or GDP is bound at MT ends.

The above results have been taken into account in an alternative model. The corresponding steady-state theory has been developed by Hill and Carlier (20) for one end, presumably the fast-growing end, called α. In developing the theory, we have assumed that (*i*) all dimeric tubulin in solution is tubulin-GTP [GTP exchanges rapidly for GDP on dimeric tubulin (21, 22)]; (*ii*) the rate constant of association of tubulin-GTP to a polymer end having GDP bound, α_{1D}, is zero, as suggested by experimental results; (*iii*) a MT consists of five independent helices; and (*iv*) κ, the hydrolysis rate constant on the MT, is relatively small (we take $\kappa = 0$ for mathematical purposes).

In comparing the steady-state theory with experiment, a complication arises. The theory provides true steady-state properties of the polymer (i.e., properties not dependent on time). On the other hand, in dilution experiments the initial rate of polymerization or depolymerization after dilution does not relate to polymer ends at a true steady state (i.e., the ends are in a transient). Monte Carlo calculations have been developed to investigate this point (23). Such calculations simulate a dilution experiment (at constant tubulin concentration) on the computer. They have shown that, in the present model, the rate of depolymerization following dilution of steady-state MTs increases with time from a low val-

The publication costs of this article were defrayed in part by page charge payment. This article must therefore be hereby marked "*advertisement*" in accordance with 18 U.S.C. §1734 solely to indicate this fact.

Abbreviations: p[NH]ppG, guanylyl imidodiphosphate; Mes, 2-morpholinoethanesulfonic acid; MT, microtubule.

ue (characteristic of the GTP-tubulin exchanges at the capped ends of MTs at $c = c_c$) to the higher value given by the steady-state theory (characteristic of the new steady state at the considered concentration c').

In the experiments described here, MTs have been diluted into solutions of dimeric tubulin at different concentrations, and the rate of polymerization (positive or negative) has been measured a few seconds after dilution. The $J_{on}(c)$ plot obtained exhibits a dramatic change in slope at c_c, in agreement with the theory; in addition, the shape of the negative branch of $J_{on}(c)$ is similar to the shape of the transient $J_\alpha(c)$ plots computed by the Monte Carlo method. Data could be fitted by a typical transient calculated using a rate constant for GDP-tubulin dissociation from MTs about 600-fold larger than that of GTP-tubulin. In conclusion, this theory in its steady-state and kinetic aspects, and the experiments that support it, apparently account for the reported disagreement between the values found experimentally for the association–dissociation rate constants and expected values compatible with the critical concentration. The implications of this peculiar behavior for the events of cell motility are discussed.

METHODS

The experimental plot $J_{on}(c)$ was obtained by diluting steady-state MTs into buffer containing different concentrations of dimeric tubulin and measuring the initial rate of the subsequent change in turbidity at 350 nm. The initial concentration of dimeric tubulin after dilution was deduced from the dilution factor, the concentration of added tubulin, and the critical concentration under the chosen experimental conditions. The critical concentration c_c was obtained independently by totally depolymerizing at 4°C MTs that had reached steady state after dilution from a MT stock solution to different concentrations. The extent of turbidity change on total depolymerization was then plotted versus total tubulin concentration, leading to determination of the critical concentration.

Protein concentration was determined either spectrophotometrically using an extinction coefficient $A^{0.1\%}_{278\ nm}$ for tubulin of 1.2 $mg^{-1} \cdot cm^2$ (24) or by the Lowry method (25) with a slight correction for tubulin.

Experiments were done using either whole MT protein obtained by three cycles of polymerization according to Shelanski *et al.* (26) or pure tubulin further purified by phosphocellulose chromatography (27). In the former case, MT protein was equilibrated (by chromatography over Sephadex G-25) and polymerization experiments were carried out in 0.1 M 2-morpholinoethanesulfonic acid (Mes) buffer pH 6.6/0.5 mM magnesium acetate/1 mM EGTA/0.1 mM GTP/20 mM acetyl phosphate containing acetate kinase (0.1 unit/ml; Sigma) as a GTP-regenerating system (28). In the latter case, the experiments were carried out in the usual pure tubulin polymerization buffer (4) consisting of 50 mM Mes, pH 6.6/0.5 mM EGTA/6 mM magnesium acetate/3.4 M glycerol/1 mM GTP. This amount of GTP was found sufficient to maintain the steady state of preformed MTs at least for the duration of the experiment. That is, the concentration of GDP eventually formed in the stock MT solution was less than 0.2 mM, which ensured a ratio of reduced GTP and GDP concentrations always higher than 10. The MT solution was diluted in tubulin solutions containing 1 mM GTP also. The tubulin solution was preequilibrated at 30°C for 1 to 2 min before dilution, and its concentration was always low enough to ensure that no nuclei were formed during the equilibration process. MTs were diluted in a thermostated cell (optical path, 1 cm; vol, 0.4 ml) and placed in a Perkin–Elmer Lambda 1 spectrophotometer connected to an Ifelec EL 15 recorder (time constant, 0.1 sec). The time base could be varied from 1 sec/cm to 20 sec/cm. The dead time caused by mixing the MTs with buffer or tubulin solutions was 3–5 sec. The absorbance scale could be increased up to 0.002 absorbance unit/cm, with noise weaker than 0.0005 absorbance unit. MTs (polymerized tubulin at 14–25 μM) were diluted with buffer or with known tubulin solutions. The mixing was made by aspiring the solution twice in an Eppendorf pipet equipped with a tubing large enough to avoid shearing of MTs and to ensure reproducibility of the MT number concentration in the cell.

RESULTS

Fig. 1 shows a typical experimental plot, $J_{on}(c)$, obtained by diluting 1:4 (i.e., by a factor of 4) MTs formed from a solution of 22 μM pure tubulin. The critical concentration c_c determined independently, as described above, was 1.7 μM. The main observation is that this plot does not consist of a single straight line intersecting the concentration axis at $c = c_c$ but exhibits a change in slope at the critical concentration. Above c_c, J_{on} is linear in c while, below c_c, the plot reaches c_c with a slope 14-fold higher than the slope of the positive branch (the ratio of the slopes was 14–17 from the average of four experiments). In other words, MTs depolymerize much faster at $c_c - \Delta c$ than they polymerize at $c_c + \Delta c$. The same result was obtained with whole MT protein and with pure tubulin. However, experiments were technically easier and more accurate with pure tubulin, which had a higher critical concentration (1.8 μM ± 0.2 μM as compared with 0.3 μM for tubulin with MT-associated proteins). In addition, pure tubulin was free of all possible MT-bundling proteins (ref. 29; P. Huitorel and D. Pantaloni, unpublished data) whose dissociation from MTs on dilution can give a turbidity change interfering with that of the depolymerization process. Therefore, experiments were routinely done with pure tubulin.

In a control experiment, MTs polymerized and maintained in a true equilibrium state in the presence of the nonhydrolyzable analog of GTP, guanylyl imidodiphosphate (p[NH]ppG), were diluted in tubulin solutions containing p[NH]ppG. The $J_{on}(c)$ plot was linear in this case. We confirmed that, as observed previously, depolymerization of p[NH]ppG MTs is very slow (2) and further observed that the pseudo-first-order rate constants for the polymerization and depolymerization processes were identical.

Fig. 1 shows that the shape of the negative branch of the

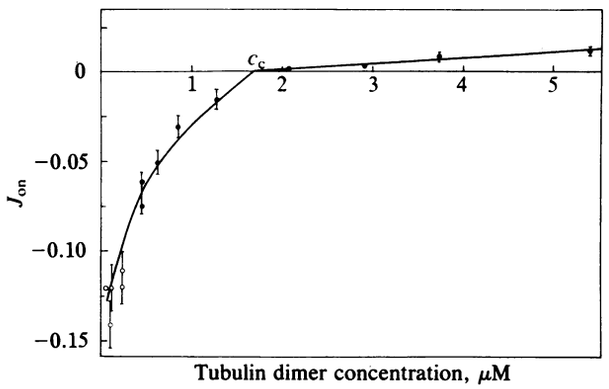

FIG. 1. Experimental $J_{on}(c)$ plot. Pure tubulin dimer at a concentration of 22 μM was polymerized into MTs and kept at steady state for at least 30 min before beginning the experiment. This solution was diluted 1:4 into tubulin dimer at a series of concentrations (●). Points at lower tubulin concentration were obtained at higher dilutions into buffer (○) and were corrected for the same MT-number concentration as for higher concentration solutions. The rate J_{on} of polymerization was measured within 3–5 sec after dilution and is expressed in absorbance units (A.U.) per min. (The turbidity of a 1 μM polymerized tubulin solution is 0.020 ± 0.002 A.U. at 350 nm.)

$J_{on}(c)$ plot differs from the theoretical curves predicted in the steady-state treatment (20). The difference is that the experimental plot is not curved upward and does not exhibit a low initial slope near $c = 0$ but rather seems to deviate slightly downward from a straight line when $c < c_c/2$. A similar observation has been made in a preliminary report (30).

There seems little doubt that the above-mentioned qualitative discrepancy is due to the fact that the experiments relate to transient conditions while the theory in ref. 20 relates to steady states. To confirm this, we have made a preliminary study of the shape of the Monte Carlo (23) theoretical transient $J_\alpha(c)$ curves. In every case that we have examined, the $J_\alpha(c)$ curves at early times after jumps in concentration values from c_α (the critical concentration of the α end) have the same curvature as observed experimentally in Fig. 1.

An explicit example is shown in Fig. 2, based on the following values of the rate constants of the model (20, 23):

$$\alpha_{1D} = 0, \quad \alpha_{1T} = 0.849, \quad \alpha_{2D} = \alpha_{2T} = 298.0$$
$$\alpha_{-1D} = \alpha_{-1T} = 0.45, \quad \kappa' = 0.060, \quad \kappa'' = 2.04$$
$$\kappa_{DD} = \kappa_{TD} = 1.0, \quad \kappa_{DT} = \kappa_{TT} = 0.002,$$

where T represents tubulin-GTP and D represents tubulin-GDP. The values are per helix and the units are sec^{-1} except $\mu M^{-1} \cdot sec^{-1}$ for α_{1T}. The rate constant κ_{DD}, for example, refers to a κ (hydrolysis) transition for an interior T with nearest neighbors D,D (23). The solid curve in Fig. 2 is the experimental curve (for $J_{on} < 0$) in Fig. 1, with the ordinate converted to units of sec^{-1} per helix. The points × in Fig. 2 are steady-state ($t = \infty$) Monte Carlo values of J_α. The critical concentration, c_α, is 2.1 μM. The broken line is the theoretical transient curve at $t = 0$, from equation 8 of ref. 23 (and confirmed by the Monte Carlo transients). Also included in Fig. 2 are Monte Carlo points for $t = 5$, 11, and 16 sec. The $t = 11$ sec points fit the experimental curve rather well (but the time scale is about three times too slow). The reason that the theoretical $J_\alpha(c)$ transients at early times have a different curvature than at $t = \infty$ (steady state) is that the fractional approach to the final $t = \infty$ value at a given c is much more rapid at small c than at large c (e.g., compare the Monte Carlo points at $c = 0$ with those at $c = 1$ μM and, especially, at 1.5 μM).

The experimental $J_{on}(c)$ plot is expected to be invariant when the MT-number concentration is changed. It was checked (Fig. 3*A*) that plots obtained through different dilutions of the same MT solution were superimposable within a range of final MT-number concentrations. This result con-

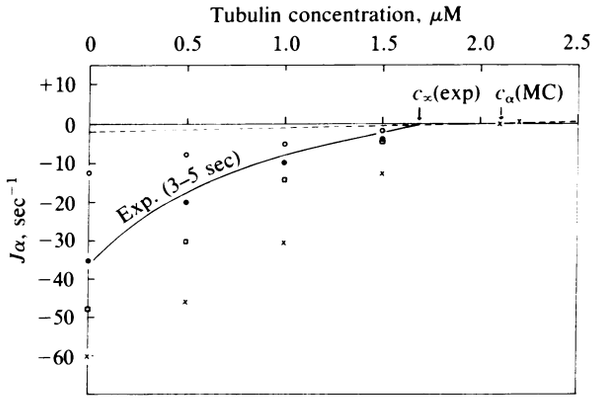

FIG. 2. Comparison of experimental $J_{on}(c)$ with Monte Carlo (MC) calculations of $J_\alpha(c)$. A change of 0.1 absorbance unit at 350 nm corresponds to the association (or dissociation) of 1560 tubulin subunits per helix (five helices per MT). --, $t = 0$ sec; ○, $t = 5$ sec; ●, $t = 11$ sec; □, $t = 16$ sec; ×, $t = \infty$.

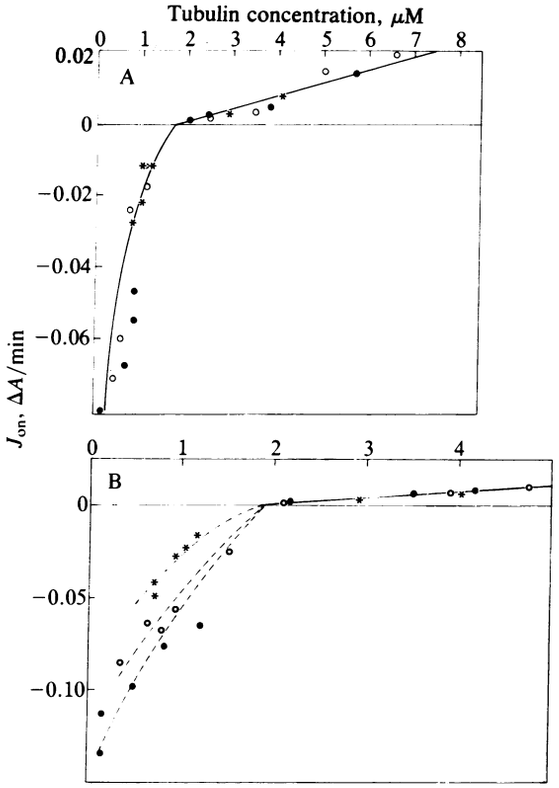

FIG. 3. $J_{on}(c)$ plots obtained from different dilutions of the same MT solution. (*A*) Stock MT solution (13.6 μM tubulin) was diluted 1:10 (●), 1:4 (○), and 1:2 (*). (*B*) Stock MT solution (30 μM tubulin) was diluted 1:10 (●), 1:5 (○), and 1:2.5 (*).

firms the above-mentioned expectation. Thus, at all dilutions the change in tubulin dimer concentration during the dead time was small enough to be neglected. However, when higher MT-number concentrations were used, the depolymerization flux increased to such an extent that the change in tubulin dimer concentration during the dead time could no longer be neglected. The kinetic process of the concentration change took place concomitantly with the relaxation process of the capped ends from the $c = c_c$ state to the nominal $c = c'$ concentration. The resulting situation, therefore, is complex, so that not even making a correction for $c' + \Delta c'$ would be correct.

Under such conditions (Fig. 3*B*), the plots obtained at lower dilutions were above the plots corresponding to larger dilutions. It should be noted that, because of the fact that the depolymerization process ($J_{on} < 0$) is so much faster than the polymerization ($J_{on} > 0$), only the lower branches of $J_{on}(c)$ cannot be superimposed: the change in c during the dead time is negligible in the upper branch of J_{on}.

DISCUSSION

The purpose of this work has been to study the interference of GTP hydrolysis in the mechanism of MT assembly. The results presented provide experimental evidence for a different kinetic behavior of MT below and above the critical concentration for assembly, which can be considered as a transition point between two regimes. In this respect, the experimental results agree with the steady-state analytical theory previously proposed (20).

The main features of the model that generate this peculiar behavior are the presence of both GTP and GDP at MT ends, because of GTP hydrolysis, and, correlatively, the fact that the kinetic (association–dissociation) parameters of tubulin at the ends are different according to whether GTP or GDP is bound. It is here observed experimentally that, below the

critical concentration, MTs depolymerize faster than expected in a reversible polymerization model, considering the rate of elongation and the value of the critical concentration. This behavior is an illustration of the role of GTP in the maintenance of the MT edifice. We have previously shown that, in the presence of very small concentrations of GTP, MTs cannot be maintained at steady state and eventually depolymerize (4). It further appears that the presence of GTP at the ends of MTs is necessary to ensure their stability. Indeed, the theory shows that, if the rate of exchange of GTP for GDP bound at the end tends toward zero, only GDP exists at the end, and the negative branch of the $J_\alpha(c)$ plot becomes steeper near the critical concentration (figure 6 of ref. 20). This indicates a high instability because a very slight decrease in tubulin concentration below the critical concentration will cause the MT to depolymerize very rapidly. This is indeed what happens experimentally when polymerization takes place in the presence of a very low concentration of GTP; as GTP is consumed and GDP accumulates in solution, more GDP (and less GTP) is bound to the ends and MTs are destabilized.

The theory (20) initially showed that the essential parameters involved in the regulation of the assembly–disassembly pattern are the rate of nucleotide exchange on tubulin present at MT ends and the ratio of the rates of addition of tubulin to GDP- and GTP-bound ends. Previous experiments (18) have indicated that this ratio is close to zero because tubulin does not bind to a GDP-bound end.

Actually, if tubulin were to bind at about the same rate to GDP and GTP ends, then the theoretical plot of polymerization rate versus tubulin concentration would be closer to the conventional straight line in which GTP hydrolysis does not interfere with the polymerization process. The experiment shown in Fig. 1 confirms that this is not the case, as previously found. Therefore, the rate of nucleotide exchange at MT ends—and thus the rate of GTP hydrolysis—appears as the most important parameter in the regulation of MT assembly-disassembly.

While the steady-state theory (20) calculated the polymer composition and rate of polymerization under time-independent conditions, the rates of polymerization are measured in kinetic experiments in which the composition of the polymer end and the tubulin concentration (to some extent) vary with time. The experimental points thus should correspond to theoretical *transient* states. After the derivation of the steady-state theory, Monte Carlo calculations of the evolution of polymer composition with time (23) have shown that, in dilution experiments, the GTP/GDP composition of MT ends undergoes a relaxation process, following a jump in concentration, eventually reaching its steady-state value. The shape of the calculated transients ($c < c_c$) shows the same downward curvature as the experimental plot. A qualitative agreement could be obtained between the data and an 11-sec transient curve.

A consequence of the deviation from linearity, near the critical concentration, in the plot of the rate of polymerization versus tubulin concentration, is that the association rate constant of tubulin to MTs cannot be calculated as the ratio of the dissociation rate constant obtained in dilution experiments to the critical concentration. This observation may also account for the discrepancies in the reported values of the dissociation rate constant (31–34), depending on whether its determination has been done far from or close to the critical concentration.

For the same reason, the treadmilling efficiency, whose value has been debated often, should probably be reformulated within the present model.

It should be pointed out that the experimental plot $J_{on}(c)$ represents the sum of association–dissociation reactions at both ends of MTs while the theoretical treatment and simulated curves are concerned with one end only. The fact that the experimental plot also exhibits a discontinuity in slope at the critical concentration suggests that the rate of polymerization at one end is predominant over the rate at the other end and/or that the critical concentrations at the ends are not very different. The former possibility is supported by data reported in the literature (35–37), showing that MT growth at one end is faster than at the other. The latter possibility implies that treadmilling efficiency is low. For the reasons set out above, this issue remains unresolved. As pointed out previously (17), MT polarity makes the structure of the β-subunit, which carries the GTP exchangeable site (38), different at the two ends, so that GTP hydrolysis could take place at one end only, and a linear $J(c)$ plot would be expected for the end at which GTP is not hydrolyzed.

From a general point of view, the fact that a steady-state polymer, behaving as described here, can depolymerize much faster slightly below the critical concentration than it polymerizes slightly above may be relevant in some motile phenomena in which the assembly–disassembly processes of large polymers are involved. It may thus be of interest to examine whether the theory developed here could apply in the cell.

APPENDIX

The analytical treatment given in ref. 20 applies when $\kappa = 0$ and $\alpha_{1D} = 0$. A similar treatment can be given in a slightly more general case: there is an uninterrupted string of N Ts from position $n = 2$ to position $n = N + 1$, inclusive, as in figure 3 of ref. 20; however, now the last T of the string, at $n = N + 1$, has a rate constant $\kappa \geq 0$ for the transition T → D. No other T in the string can make the transition.

The derivation is similar to that in ref. 20 (which is the special case $\kappa = 0$); therefore, we give only final results. The notation is the same as in ref. 20. The upper branch equation for $J_\alpha(c)$ is unchanged; it is equation 2 of ref. 20. Here it is valid for $J_\alpha > \kappa$. There is a discontinuity in the slope of $J_\alpha(c)$ at $J_\alpha = \kappa$, which occurs at $c = c_0$.

For the lower branch ($c < c_0$),

$$J_\alpha(c) = \frac{\kappa(y + z) - (\alpha_{2D} + \alpha_{-1D}x)(1 - zx^{-1})}{1 + x + y - zx^{-1}}, \quad [1]$$

where

$$x = \frac{q(v + wu - s - 2ur + \sqrt{\ })}{2[vr + (s + ur)(w - r)]}, \quad [2]$$

$$\frac{y}{x} = \frac{s - v - wu + \sqrt{\ }}{2u}, \quad [3]$$

$$\frac{z}{x} = \frac{s + v + wu - \sqrt{\ }}{2}, \quad [4]$$

$$\sqrt{\ } = [(s + v + wu)^2 - 4vs]^{1/2}$$

and

$$q = \kappa''/\kappa, \quad r = (\kappa' + \alpha_{-1D})/\kappa,$$
$$s = \alpha_{1T}c/(\alpha_{-1T} + \kappa), \quad u = (\alpha_{2T} + \kappa)/(\alpha_{-1T} + \kappa), \quad [5]$$
$$v = (\kappa + \alpha_{2T} + \kappa'')/\kappa, \quad w = \kappa'/\kappa.$$

Note that $J_\alpha = \kappa$ when $z/x = 1$. The concentration c enters through the parameter s.

The probabilities of different string types are

$$p_{DN} = \left(\frac{z}{x}\right)^{N-1} \frac{y\,(1 - zx^{-1})}{1 + x + y - zx^{-1}} \qquad (N \geq 1), \qquad [6]$$

$$p_{TN} = \left(\frac{z}{x}\right)^{N} \frac{x(1 - zx^{-1})}{1 + x + y - zx^{-1}} \qquad (N \geq 0), \qquad [7]$$

$$p_{D0} = (1 - zx^{-1})/(1 + x + y - zx^{-1}). \qquad [8]$$

The mean value of N is then

$$\bar{N} = \frac{y + z}{(1 + x + y - zx^{-1})(1 - zx^{-1})} \qquad [9]$$

and the variance is

$$\frac{\overline{N^2} - \bar{N}^2}{\bar{N}^2} = \frac{1 + x + yzx^{-1} - z^2x^{-2}}{y + z}. \qquad [10]$$

Note that $\bar{N} \to \infty$ as $z/x \to 1$.

The rate of GTP hydrolysis is

$$J_h = \frac{(y + z)\kappa + x\kappa'}{1 + x + y - zx^{-1}}. \qquad [11]$$

Finally, the concentration c_0 at which $J_\alpha = \kappa$ is

$$c_0 = \frac{(\alpha_{2T} + \kappa'')(\alpha_{-1T} + \kappa) + (\alpha_{2T} + \kappa)\kappa'}{(\alpha_{2T} + \kappa'')\alpha_{1T}}. \qquad [12]$$

1. Oosawa, F. & Kasai, M. (1971) *Biol. Macromol.* **5**, 261–322.
2. Weisenberg, R. C., Deery, W. J. & Dickinson, P. J. (1976) *Biochemistry* **15**, 4248–4254.
3. David-Pfeuty, T., Erickson, H. P. & Pantaloni, D. (1977) *Proc. Natl. Acad. Sci. USA* **74**, 5372–5376.
4. Carlier, M.-F. & Pantaloni, D. (1978) *Biochemistry* **17**, 1908–1915.
5. Carlier, M.-F. & Pantaloni, D. (1981) *Biochemistry* **20**, 1918–1924.
6. Pardee, J. D. & Spudich, J. A. (1982) *J. Cell Biol.* **93**, 648–654.
7. Mockrin, S. C. & Korn, E. D. (1982) *J. Cell Biol.* **95**, 284 (abstr.).
8. Arai, T. & Kaziro, Y. (1976) *Biochem. Biophys. Res. Commun.* **69**, 369–376.
9. Johnson, K. A. & Borisy, G. G. (1977) *J. Mol. Biol.* **117**, 1–31.
10. Wegner, A. (1976) *J. Mol. Biol.* **108**, 139–150.
11. Margolis, R. L. & Wilson, L. (1978) *Cell* **13**, 1–8.
12. Kirschner, M. W. (1980) *J. Cell Biol.* **86**, 330–334.
13. Hill, T. L. (1980) *Proc. Natl. Acad. Sci. USA* **77**, 4803–4807.
14. Hill, T. L. (1981) *Proc. Natl. Acad. Sci. USA* **78**, 5613–5617.
15. Margolis, R. L. & Wilson, L. (1981) *Nature (London)* **293**, 705–711.
16. Hill, T. L. & Kirschner, M. W. (1982) *Int. Rev. Cytol.* **78**, 1–125.
17. Carlier, M.-F. (1982) *Mol. Cell. Biochem.* **47**, 97–113.
18. Carlier, M.-F. & Pantaloni, D. (1982) *Biochemistry* **21**, 1215–1224.
19. Engelborghs, Y. & Van Houtte, A. (1981) *Biophys. Chem.* **14**, 195–202.
20. Hill, T. L. & Carlier, M.-F. (1983) *Proc. Natl. Acad. Sci. USA* **80**, 7234–7238.
21. Engelborghs, Y. & Ecckeston, J. (1982) *FEBS Lett.* **141**, 78–81.
22. Brylawski, B. P. & Caplow, M. (1983) *J. Biol. Chem.* **258**, 760–763.
23. Chen, Y. & Hill, T. L. (1983) *Proc. Natl. Acad. Sci. USA* **80**, 7520–7523.
24. Detrich, H. W., III, & Williams, R. C. (1978) *Biochemistry* **17**, 3900–3907.
25. Lowry, O. H., Rosebrough, N. J., Farr, A. L. & Randall, R. J. (1951) *J. Biol. Chem.* **193**, 265–275.
26. Shelanski, M. L., Gaskin, F. & Cantor, C. R. (1973) *Proc. Natl. Acad. Sci. USA* **70**, 765–768.
27. Weingarten, M. D., Lockwood, A. M., Hwo, S. Y. & Kirschner, M. W. (1975) *Proc. Natl. Acad. Sci. USA* **72**, 1858–1862.
28. MacNeal, R. K., Webb, B. C. & Purich, D. L. (1977) *Biochem. Biophys. Res. Commun.* **74**, 440–447.
29. Kumagai, H. & Sakai, H. (1983) *J. Biochem. (Tokyo)* **93**, 1259–1270.
30. Farrell, K. W., Himes, R. H., Jordan, M. A. & Wilson, L. (1982) *J. Cell Biol.* **95**, 351 (abstr.).
31. Farrell, K. W., Kassis, J. A. & Wilson, L. (1979) *Biochemistry* **18**, 2642–2647.
32. Bergen, L. G. & Borisy, G. G. (1980) *J. Cell Biol.* **84**, 141–150.
33. Karr, T. L., Kristofferson, D. & Purich, D. L. (1980) *J. Biol. Chem.* **255**, 8560–8566.
34. Farrell, K. W. & Jordan, M. A. (1982) *J. Biol. Chem.* **257**, 3131–3138.
35. Dentler, W., Granett, S., Witman, G. B. & Rosenbaum, J. L. (1974) *Proc. Natl. Acad. Sci. USA* **71**, 1710–1714.
36. Allen, C. & Borisy, G. G. (1974) *J. Mol. Biol.* **90**, 381–402.
37. Summers, K. & Kirschner, M. W. (1979) *J. Cell Biol.* **83**, 205–217.
38. Geahlen, R. L. & Haley, B. E. (1977) *Proc. Natl. Acad. Sci. USA* **74**, 4375–4377.